J. Math. Biol. (2009) 59:105–122
DOI 10.1007/s00285-008-0221-z

Mathematical Biology

Phytoplankton depth profiles and their transitions near the critical sinking velocity

Theodore Kolokolnikov · Chunhua Ou · Yuan Yuan

Received: 25 February 2008 / Revised: 4 July 2008 / Published online: 16 September 2008

Abstract We consider a simple phytoplankton model introduced by Shigesada and Okubo which incorporates the sinking and self-shading effect of the phytoplankton. The amount of light the phytoplankton receives is assumed to be controlled by the density of the phytoplankton population above the given depth. We show the existence of non-homogeneous solutions for any water depth and study their profiles and stability. Depending on the sinking rate of the phytoplankton, light intensity and water depth, the plankton can concentrate either near the surface, at the bottom of the water column, or both, resulting in a "double-peak" profile. As the buoyancy passes a certain critical threshold, a sudden change in the phytoplankton profile occurs. We quantify this transition using asymptotic techniques. In all cases we show that the profile is locally stable. This generalizes the results of Shigesada and Okubo where infinite depth was considered.

Keywords Phytoplankton · Depth · Stability

Mathematics Subject Classification (2000) 65L10 · 92B05 · 35B32 · 35B40

T. Kolokolnikov (✉)
Department of Mathematics and Statistics, Dalhousie University,
Halifax, NS, Canada B3H 3J5
e-mail: tkolokol@mathstat.dal.ca; tkolokol@gmail.com

C. Ou · Y. Yuan
Department of Mathematics and Statistics,
Memorial University of Newfoundland, St John's, NF, Canada A1C 5S7
e-mail: ou@math.mun.ca

Y. Yuan
e-mail: yyuan@math.mun.ca

1 Introduction

Since the classical work of Riley [16], many mathematical models of phytoplankton have been proposed, see for example [1,3,5,7–9,11,15,17]. These papers study the formation of phytoplankton blooms from the mathematical, experimental and numerical viewpoints. One of the simplest mathematical models was introduced in [17]. It takes into account light absorption by the phytoplankton. Any other nutrient and species interactions are modeled via a source term. The authors also introduced a simplifying assumption that the light absorption by water is negligible compared to the absorption by the phytoplankton itself (the so-called self-shading case). They then showed the existence of phytoplankton blooms for water columns of infinite depth, under some additional assumptions on the sinking velocity of the phytoplankton.

In this paper we analyse the self-shading model [17] for the case of finite water depth using a combination of rigorous and asymptotic techniques. We show that even a simple model can lead to complicated phytoplankton distributions. Before stating our results, let us review the model introduced in [17]; see also [3] for detailed derivation. Consider a single phytoplankton species and let $p(x,t)$ denote its population density at depth x and time t. The species is subject to diffusion, sinking and its production rate depends on light intensity. This is modeled as

$$\frac{\partial p}{\partial t} = D\frac{\partial^2 p}{\partial x^2} - v\frac{\partial p}{\partial x} + g(I)p$$

where D is the diffusivity of the plankton and v is its sinking velocity. The function $g(I(x,t))$ is the specific growth rate of phytoplankton as a function of light intensity $I(x,t)$. A standard model that incorporates saturation is

$$g(I) = \frac{aI}{1+bI} - k_d \tag{1}$$

where a and b are two positive constants and the constant k_d denote the death rate. An alternative model derived from more physical considerations (see [14,18]) is given by

$$g(I) = b\frac{1-e^{-cI}}{c} - k_d. \tag{2}$$

Light intensity I is decreasing with depth x due to light absorption via plankton and water. This is modeled by

$$\frac{dI}{dx} = -\left(k_p p + k_w\right) I$$

so that

$$I = I_0 e^{-k_w x} e^{-k_p \int_0^x p(s,t)ds}$$

where I_0 is the light intensity at the surface. The water is assumed to have the depth L. We will use a normalization $D = 1$ and obtain the following model,

$$\begin{cases} \dfrac{\partial p}{\partial t} = \dfrac{\partial^2 p}{\partial x^2} - v\dfrac{\partial p}{\partial x} + g(I)p, \quad x \in (0, L) \\ \dfrac{\partial p}{\partial x} - vp = 0, \quad \text{at } x = 0 \quad \text{and} \quad x = L, \\ I = I_0 e^{-k_w x} e^{-k_p \int_0^x p(s,t)ds}. \end{cases} \tag{3}$$

The boundary conditions reflect the fact that the plankton cannot cross the air-water or the water ground interfaces.

In general, Eq. (3) is an integral-differential equation. However, if the plankton is assumed to be sufficiently transparent (i.e. $k_p = 0$), then Eq. (3) will reduce to a completely linear model which was studied in [3] and [5] among others. In [5], Fennel found that a species occurs in highest abundance in the vertical location where its species-specific growth and loss rates are balanced, while in [3] the authors used Bessel functions to study the distribution of the plankton and their results show that the condition for phytoplankton bloom can be captured by a critical depth, a compensation depth, and zero, one or two critical values of the vertical turbulent diffusion coefficient.

Another simplification used in [17] is to assume that most of the light is absorbed by the plankton itself (i.e. $k_w = 0$). This is the so-called self-shading model and is the regime that we will study in this paper. We now summarize our results.

In Sect. 2 we rigorously study the steady state of the self-shading model for finite water depth L. We show that there exists a unique non-constant steady state for any L. This generalizes results of [17], where it was assumed that $L = \infty$. In addition we study the local stability of the non-constant solution, and show that it is indeed stable. In Sect. 3 we study the change in the solution profile as the sinking velocity v is increased. The plankton concentrates at the bottom of the water column for large enough v and near the surface if v is small. Indeed there is a critical value v_c near which the transition occurs. We use asymptotic techniques to describe this narrow transition regime.

In Sect. 4 we perform an asymptotic analysis of the Webb–Newton–Starr nonlinearity (2) in the limit where $I_0 c \gg 1$. In such a regime, the population profile can be estimated explicitly by solving a piecewise linear ODE. Depending on the water depth, we found regimes for which plankton density has two peaks, one at or near the surface, and another peak near the bottom of the water column. Such solution occurs for finite L only, and is stable both in time and in parameter space. Some open problems are discussed in Sect. 5.

2 Existence, uniqueness and stability of the steady state

2.1 Existence and uniqueness

Before deriving the results, we review the non-local transformation introduced in [17] to simplify the model in the self-shading case $k_w = 0$. After scaling, set $k_p = 1$ and let

$$Q(x, t) = \int_0^x p(s, t)ds.$$

and define

$$f(Q) = \int_0^Q g(I_0 e^{-s}) ds. \tag{4}$$

We then obtain a new equation for Q,

$$\begin{cases} Q_t = Q'' - vQ' + f(Q) \quad \text{for } x \in (0, L) \\ Q(0) = 0; \quad Q''(L) - vQ'(L) = 0 \end{cases} \tag{5}$$

In order to obtain nontrivial steady states, we shall need a further assumption that the phytoplankton has a positive growth rate at the surface; that is,

$$g(I_0) > 0. \tag{6}$$

or equivalently, $f'(0) > 0$. Since $g(Ie^{-s})$ tends to $-k_d$ as $s \to \infty$ and since $g(Ie^{-s})$ is monotone in s, we see that in this case, $f(Q)$ has precisely two positive roots at $Q = 0$ and $Q = Q_\infty$, with $f(Q)$ positive for $Q \in (0, Q_\infty)$ and with $f(Q)$ negative otherwise.

In this section we study the existence and uniqueness of the nonhomogeneous steady state of (5) and its stability. The steady state satisfies

$$\begin{cases} 0 = Q'' - vQ' + f(Q), \\ Q(0) = 0, \quad Q(L) = Q_\infty \quad \text{where } f(Q_\infty) = 0. \end{cases} \tag{7}$$

Generally speaking, the plankton will sink to the bottom of water column if its sinking velocity v is sufficiently large; it will then survive there if the reproduction rate at the bottom is greater than the death rate. On the other hand, for very light plankton such as picophytoplankton or for some species that have gas vesicles [3], v may be near zero or positive. In the case of zero velocity, the steady state reduces to

$$\begin{cases} 0 = Q'' + f(Q), \\ Q(0) = 0, \quad Q(L) = Q_\infty. \end{cases} \tag{8}$$

and an explicit solution in terms of quadrature is available. In particular for the case of deep water column ($L = \infty$), the plankton density at the surface is given by

$$p(0) = Q'(0) \sim \sqrt{2 \int_0^{Q_\infty} f(s) ds} \tag{9}$$

and $p(x)$ decays exponentially to 0 as $x \to \infty$.

Here we are primarily concerned with the regime where v is positive but not too large. In this case, surface or subsurface concentrations may occur. This coincides with the fact that maxima of phytoplankton biomass often occurs *in* clear water, not necessarily on the surface, in oceans and in lakes (for example, see [2,16]). In [17], the authors have proved the existence of a non-homogeneous steady state in the case of infinite depth ($L = \infty$) under an additional restriction on v. In this section we extend these results for the case of the finite depth. We also prove that this equilibrium is locally stable. Our existence result is the following.

Theorem 2.1 *Suppose that* $f'(0) > 0,\ f'(Q_\infty) < 0$. *Then the solution to* (7) *exists for any* $v \geq 0,\ 0 < L < \infty$, *and is unique. If* $L = \infty$, *then the solution to* (7) *exists provided that* $v < v_c$ *where*

$$v_c = 2\sqrt{f'(0)}. \tag{10}$$

When $L = \infty$, the existence of the steady state was shown in [17] using phase plane analysis. In this case, the solution to (7) lies on a heteroclinic orbit that connects the unstable equilibrium at $Q = 0$ to the saddle point at $Q = Q_\infty$. Here, we extend the results in [17] for the case when L is finite. As in [17], the existence follows from phase plane analysis. The main difficulty here is to prove the uniqueness of solution, which requires a certain monotonicity property (Lemma 2.1 below).

We begin by reviewing the phase plane of the corresponding autonomous system,

$$\begin{cases} \dot{Q} = p, \\ \dot{p} = vp - f(Q) \end{cases} \tag{11}$$

The steady state $Q = 0,\ p = 0$ has the eigenvalues

$$\lambda = \frac{v \pm \sqrt{v^2 - 4f'(0)}}{2}.$$

Since $f'(0) > 0$, this is an unstable equilibrium which is a spiral (i.e. complex conjugate eigenvalues) when $0 < v < v_c = 2\sqrt{f'(0)}$. On the other hand when $v > v_c$, the eigenvalues are purely real. The other equilibrium is $Q = Q_\infty,\ p = 0$ and has eigenvalues

$$\lambda = \frac{v \pm \sqrt{v^2 - 4f'(Q_\infty)}}{2}.$$

Since $f'(Q_\infty) < 0$, this is a saddle point. Now from the sketch of the phase plane (see Fig. 1), there is a heteroclinic connection between the unstable manifold of $Q = 0$ and the stable manifold of $Q = Q_\infty$ when $v > 0$. If $0 < v < v_c$, the origin is a spiral so that the heteroclinic orbit crosses the positive p-axis as shown at some point $p = p_c$, as shown on Fig. 1a. This orbit is precisely the solution to (7) in the case $L = \infty$.

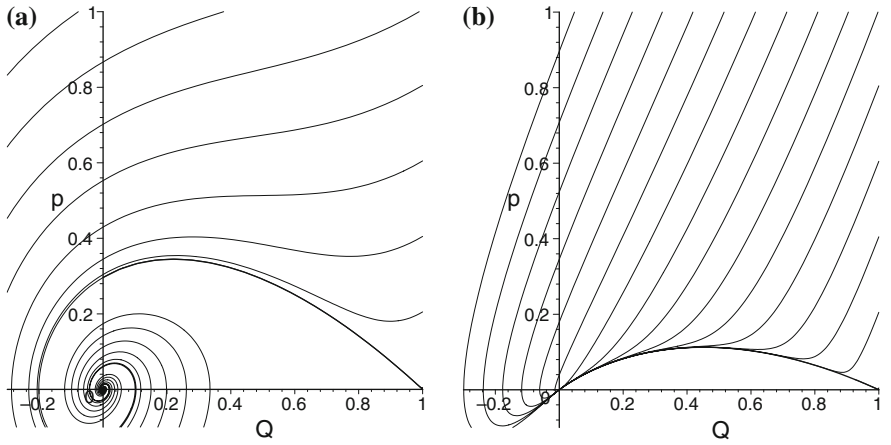

Fig. 1 Phase plots of system (11) with $f(Q) = Q - Q^2 \implies v_c = 2$. **a** $v = 0.2 < v_c$. The *thick curve* corresponds to the solution of (7) that corresponds to $L = \infty$. It lies on a heteroclinic orbit connecting $Q = 1$ to $Q = 0$. **b** $v = 2.2 > v_c$. The *thick curve* corresponds to a heteroclinic orbit

To prove the existence and uniqueness of solution for finite L, we consider the corresponding initial value problem

$$\begin{cases} 0 = Q'' - vQ' + f(Q), \\ Q(0) = 0, \quad Q'(0) = \mu. \end{cases} \tag{12}$$

We show the following key monotonicity result.

Lemma 2.1 (a) *Given* $0 < \mu_1 < \mu_2$, *let* Q_{μ_1} *and* Q_{μ_2} *be two positive solutions of* (12). *Then* $Q_{\mu_1}(x) < Q_{\mu_2}(x)$ *for all* $x > 0$.

(b) *Let* $p_c = Q'(0)$ *where* Q *is the solution to* (7) *corresponding to* $L = \infty$. *If* $\mu > p_c$ *then* $Q_\mu(x)$ *is an increasing function for all* x.

Proof (a) Since f' is bounded on $[0, Q_\infty]$, we may choose a constant $k > \max_{Q\in[0,Q_\infty]} |f'(Q)|$. Next define

$$f_0(Q) = f(Q) + kQ.$$

From the choice of k, it is clear that $f_0(Q)$ is increasing on $[0, Q_\infty]$ and $f_0(Q) \geq 0$ on $[0, Q]$. Next rewrite the first equation of (7) as

$$Q'' - vQ' - kQ = -f_0(Q).$$

Using the initial conditions in (12) we can construct an equivalent integral equation for Q:

$$Q_\mu(x) = \mu\left(\frac{e^{\lambda_1 x} - e^{\lambda_2 x}}{\lambda_1 - \lambda_2}\right) + \frac{1}{(\lambda_1 - \lambda_2)}\int_0^x \left(e^{\lambda_1(x-s)} - e^{\lambda_2(x-s)}\right) f_0(Q)ds, \tag{13}$$

$$\lambda_1 = \frac{v + \sqrt{v^2 + 4k}}{2}, \quad \lambda_2 = \frac{v - \sqrt{v^2 + 4k}}{2}.$$

Since $Q'_\mu(0) = \mu$, there exists a small neighborhood near $x = 0$ such that $Q_{\mu_1}(x) > Q_{\mu_2}(x)$ in that neighborhood. Now suppose that $Q_{\mu_2}(x) \le Q_{\mu_1}(x)$ for some $x > 0$. Then there exists x_0 so that $Q_{\mu_2}(x) > Q_{\mu_1}(x)$ if $x \in [0, x_0)$ but $Q_{\mu_1}(x_0) = Q_{\mu_2}(x_0)$. But then we have

$$\begin{aligned} Q_{\mu_2}(x_0) - Q_{\mu_1}(x_0) = (\mu_2 - \mu_1)&\left(\frac{e^{\lambda_1 x_0} - e^{\lambda_2 x_0}}{\lambda_1 - \lambda_2}\right) \\ &+ \frac{1}{(\lambda_1 - \lambda_2)}\int_0^{x_0} \left(e^{\lambda_1(x_0-s)} - e^{\lambda_2(x_0-s)}\right) \\ &\times \left[f_0(Q_{a_2}(s)) - f_0(Q_{a_1}(s))\right] ds. \end{aligned} \tag{14}$$

Now the first term on the right hand side is strictly positive since $\mu_2 > \mu_1$ and $\lambda_1 > \lambda_2$. On the other hand, $f_0(Q_{\mu_2}(s)) - f_0(Q_{\mu_1}(s)) > 0$ for all $s \in [0, x_0]$ since $Q_{\mu_2}(s) > Q_{\mu_1}(s)$ and since f_0 is increasing. Therefore the integral term is also positive and so the right hand side is strictly positive. On the other hand, the left hand side is zero by since we assumed $Q_{\mu_1}(x_0) = Q_{\mu_2}(x_0)$. We obtain a contradiction. This completes the proof of (a).

The statement (b) follows easily from the analysis of the phase plot of (11)—see Fig. 1. We omit the details. □

Proof of Theorem 2.1 Define a function $L = L(\mu)$ to be such that $Q_\mu(L) = Q_\infty$. where Q_μ is the solution to (12). Due to continuous dependence of (12) on μ, it is clear that $L(\mu)$ is a continuous function of μ. Moreover, $L \to \infty$ as $\mu \to p_c$. On the other hand, for large μ, the solution to (12) is estimated asymptotically by a system

$$0 \sim Q'' - vQ', \quad Q(0) = 0, \quad Q'(0) = \mu \gg 1$$

whose solution is given by

$$Q_\mu(x) \sim \frac{\mu}{v}\left(1 - e^{-vx}\right), \quad \mu \gg 1.$$

From this we obtain

$$Q_\infty \sim \frac{\mu}{v}\left(1 - e^{-vL}\right), \quad \mu \gg 1.$$

so that

$$L \sim \frac{Q_\infty}{\mu}, \quad \mu \gg v.$$

Therefore, $L(\mu)$ is a continuous function with $L(\mu) \to \infty$ as $\mu \to p_c^+$ and $L(\mu) \to 0$ as $\mu \to \infty$. This shows that the solution to (7) exists for any $L > 0$. Finally, Lemma 2.1 shows that L is a strictly decreasing function of μ. This shows the uniqueness of solution to (7). □

2.2 Stability

Next we show that the steady state constructed in Theorem 2.1 is indeed stable. To do so, we linearize around the steady state,

$$Q(x,t) = Q(x) + \phi(x)e^{\lambda t}$$

where $Q(x)$ is the equilibrium steady as constructed in Theorem 2.1 and $\phi \ll 1$ is a small perturbation. Substituting into (5) and keeping the leading order terms we obtain the following eigenvalue problem,

$$\lambda\phi = \phi_{xx} - v\phi_x + f'(Q)\phi; \quad \phi(0) = 0; \quad \left[\lambda - f'(Q_\infty)\right]\phi(L) = 0. \tag{15}$$

Our main result is the following.

Theorem 2.2 *All eigenvalues of* (15) *are real and negative and thus the positive steady state Q is stable.*

We remark that Shigesada and Okubo [17] used a Lyapunov functional approach to prove global stability of the steady state in the case infinite L. Their approach relies on uniqueness of the steady state. For the case of *finite* L the uniqueness is shown in Theorem 2.1; indeed the rest of the proof of global stability can be carried through. Here, we use a simpler approach to show only local stability, which also works for more general systems where uniqueness may not be guaranteed.

Proof of Theorem 2.2 We first rewrite (15) to make the problem self adjoint. Define

$$L\phi \equiv \left(e^{-vx}\phi'\right)' + e^{-vx}f'(x)\phi$$

so that (15) becomes

$$\lambda e^{-vx}\phi = L\phi \tag{16}$$

The proof now consists of two steps.

Step 1: *All real eigenvalues are negative.* Note that Q' satisfies $LQ' = 0$. Multiplying both sides of (16) by Q' and integrating the right hand side by parts twice from 0 to x_0 we therefore obtain

$$\lambda \int_0^{x_0} \phi Q' e^{-vx} dx = \left[e^{-vx} \phi' Q' - \left(e^{-vx} Q' \right)' \phi \right]_{x=0}^{x=x_0}. \tag{17}$$

Now either $\lambda = f'(Q_\infty)$ or else $\phi(L) = 0$. In the former case, λ is negative and we are done. In the latter, case, let x_0 be the leftmost nonzero root of ϕ. Then (17) becomes

$$\lambda \int_0^{x_0} \phi Q' e^{-vx} dx = \left[e^{-vx} \phi' Q' \right]_{x=0}^{x=x_0}.$$

Since λ is assumed to be real, we may take $\phi > 0$ on the interval $(0, x_0)$ with $\phi(0) = \phi(x_0) = 0$ (by replacing ϕ by $-\phi$ if necessary). Then $\phi'(0) \geq 0$ and $\phi'(x_0) \leq 0$. In fact, using the strong maximum principle, one has a stronger condition $\phi'(0) > 0$ and $\phi'(x_0) < 0$, since otherwise $\phi \equiv 0$ on the whole interval $[0, L]$. Finally, $Q' > 0$ by Theorem 2.1. It immediately follows that $\lambda < 0$ provided that λ is real.

Step 2: *All eigenvalues are real*: Multiply (16) by $\bar{\phi}$ and integrate both sides on $[0, L]$. We then obtain

$$\lambda \int_0^L |\phi|^2 e^{-vx} dx = \int_0^L \overline{\phi} L \phi dx = \int_0^L \phi L \overline{\phi} dx = \overline{\int_0^L \overline{\phi} L \phi dx}$$

It follows that $\lambda \int_0^L |\phi|^2 e^{-vx} dx = \bar{\lambda} \int_0^L |\phi|^2 e^{-vx} dx$ so that λ is purely real. □

3 Population profiles near the critical sinking velocity

When plotting the phase plane for the steady state profile as was done in Theorem 2.1, it is clear that there are two distinguished cases depending on whether $v > v_c$ or $v < v_c$ where $v_c = 2\sqrt{f'(0)}$ is the critical sinking velocity at which the zero steady state has a double eigenvalue. When the water depth L is sufficiently large, the population profile concentrates near the surface for small v. However, for $v > v_c$, the heteroclinic orbit shown in Fig. 1b never intersects the positive p axis; as a result, all orbits close to the heteroclinic orbit spend a long time near the equilibrium $Q = Q_\infty$. This implies that the plankton populations concentrate at the bottom of the water column when $v > v_c$. Therefore there is a transition that occurs as v crosses v_c. An example of this phenomenon is shown in Fig. 2a. In this section we quantify this transition, in the case where the water depth is sufficiently large. Our main result is the following.

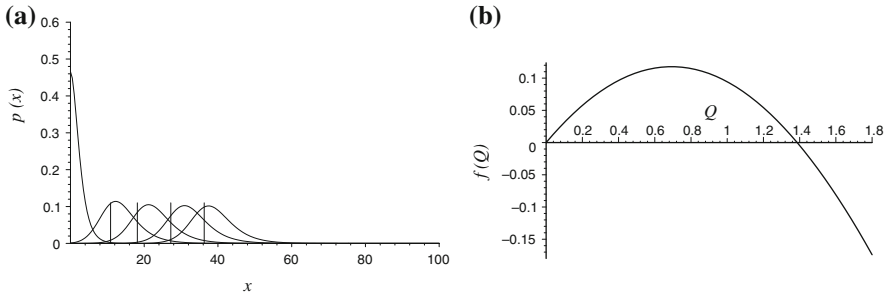

Fig. 2 Subsurface plankton populations for model (3) with nonlinearity (1). The parameters are $a = 2$, $b = 1, k_d = 1, I_0 = 2, L = 100$. **a** Profiles of plankton densities p with v given by (18) and with $\alpha = 0.15, 0.2, 0.3, 0.5, \sqrt{2}$ (from *right* to *left*). The *vertical axis* represents depth with the density $p(x)$ plotted on the *horizontal axis*. The corresponding asymptotic location x_0 of the maximum given by (19) is shown by a *horizontal line*. A good agreement is observed. **b** The plot of $f(Q)$, where f is given by (4) and (2). The critical buoyancy (10) is $v_c = 1.1547$

Proposition 3.1 *Suppose that*

$$v = \sqrt{f'(0)}\left(2 - \alpha^2\right), \quad \alpha \ll 1. \tag{18}$$

Consider the steady state profile of Theorem 2.1 and suppose that

$$L \gg O\left(\frac{1}{\alpha}\right).$$

Then the plankton population $p(x)$ has an interior maximum that is located asymptotically at

$$x_0 \sim \frac{\pi}{\sqrt{f'(0)}}\frac{1}{\alpha}. \tag{19}$$

Proof As before, we consider the steady state equations (5). Now let us rescale

$$\begin{aligned} x &= x_0 + ly \\ Q(x) &= u(y) \end{aligned}$$

where x_0 is the location of the inflection point of Q, corresponding to the maximum of p and where l will be chosen later. We obtain

$$0 = u_{yy} - vlu_y + l^2 f(u)$$

We now choose $l^2 = \frac{1}{f'(0)}$ and obtain

$$\begin{cases} 0 = u_{yy} - v_0 u_y + h(u) \\ u(-L_1) = 0, \quad u(L_2) = Q_\infty, \quad u''(0) = 0 \end{cases}$$

where

$$L_1, L_2 \gg 1; \quad h'(0) = 1$$

and

$$v_0 = -vl, \quad h(u) = f(u)\, l^2, \quad l = 1/\sqrt{f'(0)}$$
$$L_1 = \frac{x_0}{l}, \quad L_2 = \frac{L - x_0}{l}.$$

We first analyze the stability of the steady state $u = 0$. Substituting $u = 0 + e^{\lambda y} c$, $c \ll 1$ we obtain the characteristic equation $\lambda^2 - v_0\lambda + 1 = 0$. It is clear then that $v_0 = 2$ is the threshold value so that $u = 0$ is an unstable spiral for $v_0 < 2$ whereas $u = 0$ is unstable without spirals when $v_0 > 2$ and has a double eigenvalue if $v_0 = 2$. As we will show, the submerged plankton occurs when v_0 is near 2. Therefore we write

$$v_0 \equiv 2 - \alpha^2, \quad 0 < \alpha \ll 1$$

so that $\lambda \sim 1 - \alpha^2/2 \pm i\alpha$. It follows that

$$\begin{aligned} u &\sim c \exp\left(\left(1 - \alpha^2/2\right) y\right) \sin\left(\alpha\left(y + L_1\right)\right), \quad y \ll 0 \\ &\sim c \exp(y) \left[\sin(\alpha L_1) \cos(\alpha y) + \sin(\alpha y) \cos(\alpha L_1)\right]. \end{aligned}$$

In particular we have

$$u \sim c \exp(y) \left[\sin(\alpha L_1) + \alpha y \cos(\alpha L_1)\right] \quad \text{when} \quad -\frac{1}{\alpha} \ll y \ll 0. \tag{20}$$

Next, let U be the heteroclinic orbit corresponding to $v_0 = 2$ with an inflection point at $y = 0$ so that U satisfies:

$$\begin{aligned} 0 &= U_{yy} - 2U_y + h(U) \\ U &\to 0 \text{ as } y \to -\infty; \quad U \to Q_\infty \text{ as } y \to \infty \quad \text{and} \quad U''(0) = 0. \end{aligned} \tag{21}$$

Note that the equilibrium $U = 0$ has a double eigenvalue so that

$$U \sim \exp(y)\left(A + By\right), \quad y \to -\infty \tag{22}$$

for some $O(1)$ constants A and B that are independent of L_1, α. These constants are determined by solving numerically the problem (21).

Matching (20) and (22) we then obtain

$$\alpha^{-1} \tan(\alpha L_1) \sim \frac{A}{B}, \quad \alpha \to 0.$$

Since A/B is independent of α, we obtain that $\alpha L_1 \sim \pi n + \alpha B/A$, $\alpha \to 0$. Moreover u must be positive so that $\sin((L_1 + y)\alpha) \neq 0$ for $-L_1 < y \ll 0$. This yields

$$L_1 \sim \frac{\pi}{\alpha} + A/B, \quad \alpha \to 0.$$

In the original variables we therefore get (19). □

Figure 2 provides an illustration of Proposition 3.1. It demonstrates that the maximum of the profile moves to the right as α^{-1} increases, according to the law (19).

4 Population profiles with two peaks

In this section we demonstrate the existence of population profiles that consist of two peaks—one at the bottom of the water column and one near the surface. To do so, we will study in detail a piecewise-linear model of the form

$$\begin{cases} Q'' - vQ' + f(Q) = 0 \\ Q(0) = 0, \quad Q(L) = \mu_0 \end{cases} \tag{23}$$

where $f(Q)$ is a piecewise linear function that has two roots at 0 and μ_0, and the phytoplankton population is $P = \frac{dQ}{dy}$. By scaling and relabeling L and v, we will assume without loss of generality that $f(Q)$ is of the form

$$f(Q) = \begin{cases} Q, & 0 \le Q \le 1 \\ \dfrac{1}{\mu_0 - 1}(\mu_0 - Q), & 1 \le Q \le \mu_0 \end{cases}; \quad \mu_0 > 1 \tag{24}$$

In other words, $f(Q)$ is a unique piecewise linear function that connects $(0, 0)$, $(1, 1)$ and $(\mu_0, 0)$. This model is actually an approximation of the Webb-Newton-Starr nonlinearity (2) in the limit where $I_0 c \gg 1$ (up to rescaling and relabeling of constants) as we now show. Note from (2) and (4) that

$$f'(Q) = \frac{b}{c}\left(1 - e^{-cI_0 \exp(-Q)}\right) - k_d.$$

Therefore in the limit $cI_0 \gg 1$ we have

$$f'(Q) \sim \begin{cases} \dfrac{b}{c} - k_d, & Q \ll Q_0 \\ -k_d, & Q \gg Q_0 \end{cases}, \quad Q_0 \equiv \ln(cI_0) \gg 1.$$

Since f' is asymptotically piecewise constant, f can be approximated by a piecewise linear function in this limit. This is demonstrated in Fig. 3 where $f(Q)$ and its linear approximation are plotted.

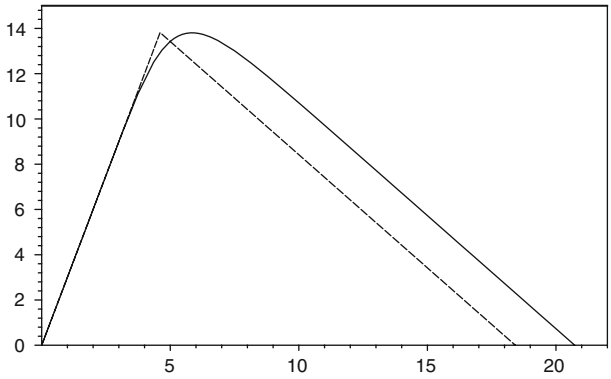

Fig. 3 The nonlinearity f given by (4) where g is given by (2). The parameter values there are $c = 100,\ b = 400,\ I_0 = 1,\ k_d = 1$. The piecewise linear approximation shown in dashes connects the points $(0,0),\ (Q_0, Q_0\left(\frac{b}{c} - k_d\right))$ and $(Q_1, 0)$ where $Q_0 = \ln(cI_0)$ and $Q_1 = Q_0 \frac{b}{ck_d}$

In terms of the nonlinearity (2), we have

$$\mu_0 \sim \frac{b}{ck_d}. \tag{25}$$

As in Section 2, the steady state $Q = 0$ admits two eigenvalues that are complex conjugate when $v < 2$ and are purely real if $v > 2$. In the latter case, the steady state will concentrate near $x = L$. However, when $v < 2$, it is possible to obtain solutions which concentrate both at the surface $x = 0$ and near the bottom $x = L$. Our goal is to demonstrate the following asymptotic result.

Proposition 4.1 *Let $p = Q'$ be the population density where Q is given by (23) with f given by (24). Suppose that*

$$L \gg 1, \quad \mu_0 \leq O(L),$$

and suppose that

$$v \gg O(\mu_0^{-1/2}) \quad \text{with } 0 < v < 2.$$

If $\mu_0 = O(L)$ then the phytoplankton profile P has two peaks, one near the bottom $x = L$ and another at $x \sim M < L$, where M is independent of μ_0, given by (28). The population concentrations at the two peaks are given by

$$p(M) \sim \frac{1}{v}; \quad p(L) \sim \mu_0 v \exp\left(-\frac{L - M}{v\mu_0}\right). \tag{26}$$

Moreover

$$p(L) \sim \mu_0 v \quad \text{when } \mu_0 \gg L.$$

Examples of such profiles are shown on Fig. 4. Since we assumed $L \gg 1$, the two-peak distribution occurs when $\mu_0 \gg 1$. In particular from (25), this can occur for

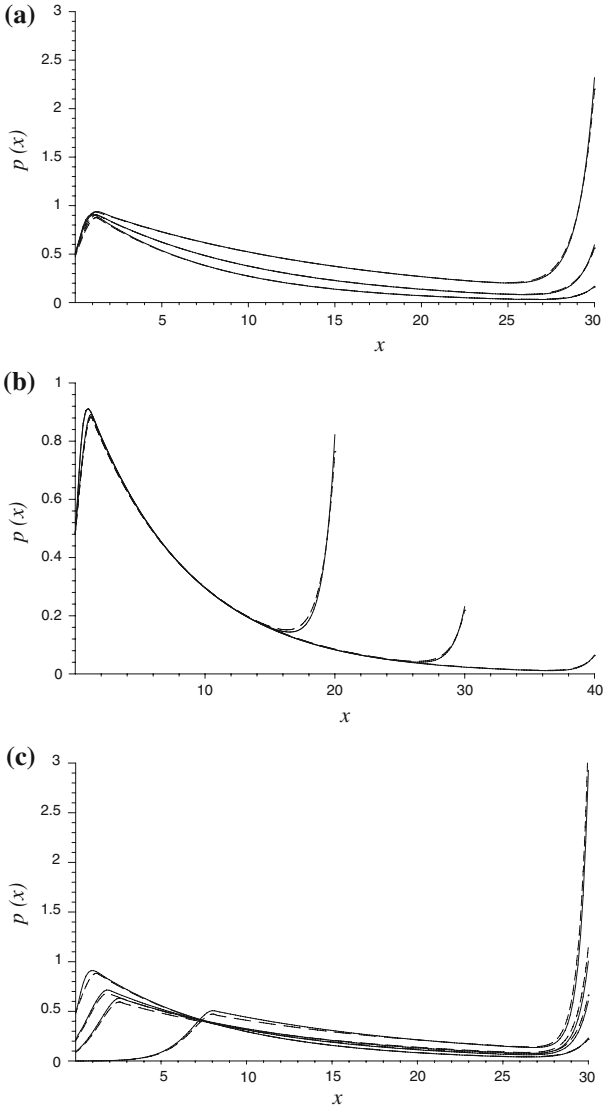

Fig. 4 Population profiles for the model (24). The *vertical axis* represents depth x with the density $p(x)$ plotted on the *horizontal axis*. *Solid curves* represent exact numerical solution; *dashed curves* represent the asymptotic solution given by (27). **a** The effect of μ_0. Parameter values are $L = 30$, $v = 1$ and $\mu_0 = 7.5, 10, 15$ (from *bottom* to *top*). **b** The effect of L with $\mu_0 = 8$, $v = 1$ and $L = 20, 30, 40$. **c** The effect of v with $\mu_0 = 8$, $L = 30$ and $v = 1, 1.3, 1.5$ and 1.9

low death rates k_d, high surface illumination I_0 as well as positive sinking velocity v. This phenomenon is illustrated in Fig. 4a. The parameter values were $L = 30$, $v = 1$, $\mu_0 = 7.5$, 10 and 15. As μ_0 is increased, a population spike appears near the bottom $x = L$, and coexists with another spike near the surface.

We now give a derivation of Proposition 4.1. Near the surface of the water column we have

$$Q \sim Q_s \sim A \exp\left(\frac{v}{2}x\right) \sin(\alpha x), \quad Q \leq 1$$

where

$$\alpha = \sqrt{1 - \frac{v^2}{4}}$$

and where A is to be determined. In this way, the condition $Q(0) = 0$ is satisfied. On the other hand, near the bottom when $Q \geq 1$ we have

$$Q_b = \mu_0 + B\left[\exp(\lambda_+ (x - L)) - \exp(\lambda_- (x - L))\right]$$

where B is to be determined; the condition $Q(L) = \mu_0$ is then automatically satisfied. The constants $\lambda_\pm$ satisfy the characteristic equation

$$\lambda^2 - v\lambda - \frac{1}{\mu_0 - 1} = 0$$

so that

$$\lambda_+ \sim v, \quad \lambda_- \sim -\frac{1}{v\mu_0} \quad \text{for } \mu_0 \gg 1.$$

To determine A, B we must glue Q_s and Q_b and their derivatives at some point $x = M$. We then obtain the following set of equations:

$$A \exp\left(\frac{v}{2}M\right) \sin(\alpha M) = 1 = \mu_0 + B\left[\exp(-\lambda_+ d) - \exp(-\lambda_- d)\right];$$

$$\frac{v}{2} + \alpha \frac{\cos \alpha M}{\sin \alpha M} = B\left[\lambda_+ \exp(-\lambda_+ d) - \lambda_- \exp(-\lambda_- d)\right]$$

where

$$d = L - M.$$

so that

$$A \exp\left(\frac{v}{2}M\right) \sin(\alpha M) = 1 = \mu_0 + B\left[\exp(-vd) - \exp\left(\frac{1}{v\mu_0}d\right)\right];$$

$$\frac{v}{2} + \alpha \frac{\cos \alpha M}{\sin \alpha M} = B\left[v \exp(-vd) + \frac{1}{v\mu_0} \exp\left(\frac{1}{v\mu_0}d\right)\right].$$

Under the assumption $v \gg \frac{1}{\sqrt{\mu_0}}$ the system simplifies to

$$\mu_0 \sim B \exp\left(\frac{1}{v\mu_0} d\right); \quad \frac{v}{2} + \alpha \frac{\cos \alpha M}{\sin \alpha M} \sim \frac{1}{v} \frac{\mu_0 - 1}{\mu_0}$$

In summary we obtain

$$Q(x) \sim \begin{cases} \exp\left(\frac{v}{2}(x - M)\right) \frac{\sin(\alpha x)}{\sin(\alpha M)}, \ 0 \le x \le M \\ \mu_0 + \mu_0 \exp\left(-\frac{L - M}{v\mu_0}\right) \left[\exp(v(x - L)) - \exp\left(-\frac{1}{\mu_0 v}(x - L)\right)\right], \\ M \le x \le L \end{cases} \tag{27}$$

where

$$\tan \alpha M \sim \frac{\alpha}{\frac{1}{v} - \frac{v}{2}}, \quad \alpha = \sqrt{1 - v^2/4}. \tag{28}$$

Recalling that $p = Q'$; equations (26) are a direct consequence of (27) and (28).

Note that the expression for M and the concentration of plankton near the surface are independent of the domain length L. Figure 4b shows the effect of the depth L on the shape of the plankton profile. It is clear that the shape of the phytoplankton near the surface is unaffected by changing L. On the other hand, changing v affects the entire profile as Fig. 4c demonstrates. Note that for values of v close to 2, we have $\alpha \ll 1$ and (28) reduces to

$$\tan \alpha M = -2\alpha; \quad \alpha \ll 1$$

so that

$$M \sim \frac{\pi}{\alpha}.$$

In fact this is a special case of Proposition 3.1 where v was assumed to be close to v_c. In this case, $p(L) = Q'(L)$ is significant provided that μ_0 is large enough, that is

$$\frac{L - \frac{\pi}{\alpha}}{2\mu_0} \ll 1.$$

5 Discussion

In this paper we have analyzed the self-shading model introduced by Shigesada and Okubo [17] for the case of finite depth L. We proved the existence and uniqueness of the steady state profile for all L. In addition, we made a more detailed analysis of the nonlinearity (2) in a certain limit. There are several open questions that remain.

In Sect. 3 we have shown that by choosing v sufficiently close to v_c, it is possible that population profiles concentrate at any given depth, under the self-shading assumption. While such solution is locally stable in time, it occurs for a rather narrow parameter range (see Proposition 3.1). As v is continuously increased past v_c, there is a very sudden change in plankton profile from surface to bottom location. This phenomenon has been observed previously in lakes; see for example [13] and [19].

An alternative mechanism for existence of subsurface peaks is the so-called deep chlorophyll maximum, see for example [1,5,6,10,12]. This can develop from the interplay between nutrient and light limitation. Incident solar light enters the water column from above, while nutrients are generally mixed upwards from deeper water layers below. Because phytoplankton growth requires both nutrients and light, a subsurface maximum often develops at an intermediate depth where the growth rate shifts from nutrient limitation to light limitation. In the tropical and subtropical oceans, this deep chlorophyll maximum typically develops at about 100 m deep.

In Sect. 4 we have studied solutions with two distinct peaks—one near the top, another at the bottom. Such distributions have been observed in lakes, see for example [4] and [13,19]. A related model that also leads to bi-stable configurations was studied in [19]. To get precise analytical results, we have considered a limiting regime of the Webb-Newton-Starr nonlinearity (2). However, numerical simulations (not shown) as well as phase plane considerations indicate that this phenomenon is in fact generic, provided certain assumptions on nonlinearity are satisfied. For the Webb-Newton-Starr nonlinearity (2) , we were able to obtain double-peaked population profile under the assumptions of high surface illumination, low death rates, positive sinking velocity and sufficiently small depth. These are all biologically plausible assumptions and we expect a possible bi-stable profile under these conditions, regardless of the precise form of the nonlinearity. We also found such profile to be relatively robust to small perturbations in parameter space. A possible physical explanation is that the production of new phytoplankton occurs predominantly near the surface. At the same time, phytoplankton continuously sinks to the bottom. In a shallow lake with sufficient illumination, this can lead to another population spike at the bottom, resulting in a bi-stable configuration.

Acknowledgments We are grateful to anonymous referees for helpful comments which improved the paper. The authors are supported by NSERC discovery grants, Canada.

References

1. Britton NF, Timm U (1993) Effects of competition and shading in planktonic communities. J Math Biol 31:655–673
2. Cullen JJ (1982) The deep chlorophyll maximum: comparing vertical profiles of chlorophyll. Can J Fish Aquat Sci 39:791–803
3. Ebert U, Arrayas M, Temme N, Sommeijer B, Huisman J (2001) Critical condition for phytoplankton Blooms. Bull Math Biol 63:1095–1124
4. Fasham MJ, Holligan PM, Pugh PR (1983) The spatial and temporal development of the spring phytoplankton bloom in the Celtic Sea. Prog Oceanogr 12:87–145
5. Fennel K (2003) Subsurface maxima of phytoplankton and chlorophyll: steady-state solutions from a simple model. Limnol Oceanogr 48:1521–1534
6. Hodges BA, Rudnick DL (2004) Simple models of steady deep maxima in chlorophyll and biomass. Deep-Sea Res I 51:999–1015

7. Huisman J, Arrayas M, Ebert U, Sommeijer B (2002) How do sinking phytoplankton species manage to persist? Am Nat 159(3):245–254
8. Huisman J, van Oostveen P, Weissing FJ (1999) Critical depth and critical turbulence: two different mechanisms for the development of phytoplankton blooms. Limnol Oceanogr 44(7):1781–1787
9. Huisman J, Sharples J, Stroom J, Visser PM, Kardinaal WEA, Verspagen JMH, Sommeijer B (2004) Changes in turbulent mixing shift competition for light between phytoplankton species. Ecology 85:2960–2970
10. Huisman J, Pham Thi NN, Karl DM, Sommeijer B (2006) Reduced mixing generates oscillations and chaos in the oceanic deep chlorophyll maximum. Nature 439:322–325
11. Ishii H, Takagi I (1982) Global stability of stationary solutions to a nonlinear diffusion equation in phytoplankton dynamics. J Math Biol 16:1–24
12. Klausmeier CA, Litchman E (2001) Algal games: the vertical distribution of phytoplankton in poorly mixed water columns. Limnol Oceanogr 46:1998–2007
13. Miracle MR, Vicente E (1983) Vertical distribution and rotifer concentrations in the chemocline of meromictic lakes. Hydrobiologia 104:259–267
14. Platt T, Gallegos CL, Harrison WG (1980) Photoinhibition of photosynthesis in natural assemblages of marine phytoplankton. J Mar Res 38:687–701
15. Reynolds CS (1984) The ecology of freshwater phytoplankton. Cambridge University Press, Cambridge
16. Riley GA, Stommel H, Bumpus DF (1949) Quantitative ecology of the plankton of the western North Atlantic. Bull Bingham Oceanogr Coll 12:1–169
17. Shigesada N, Okubo A (1981) Analysis of the self-shading effect on algal vertical distribution in natural waters. J Math Biol 12:311–326
18. Webb WL, Newton M, Starr D (1974) Carbon dioxide exhange of Alnus rubra: a mathematical model. Oceologia 17:281–291
19. Yoshiyama K, Nakajimaz H (2002) Catastrophic transition in vertical distributions of phytoplankton: alternative equilibria in a water column. J theor Biol 216:397–408